

論文 / 著書情報
Article / Book Information

Title	A computational search for wurtzite-structured ferroelectrics with low coercive voltages
Authors	Hiroki Moriwake, Rie Yokoi, Ayako Taguchi, Takafumi Ogawa, Craig A. J. Fisher, Akihide Kuwabara, Yukio Sato, Takao Shimizu, Yosuke Hamasaki, Hiroshi Takashima, Mitsuru Itoh
Citation	APL Materials, Vol. 8, Issue 12, p. 121102
Pub. date	2020, 12
Creative Commons	Information is in the article.

A computational search for wurtzite-structured ferroelectrics with low coercive voltages

Cite as: APL Mater. 8, 121102 (2020); <https://doi.org/10.1063/5.0023626>

Submitted: 03 August 2020 . Accepted: 15 November 2020 . Published Online: 07 December 2020

 Hiroki Moriwake, Rie Yokoi, Ayako Taguchi, Takafumi Ogawa,  Craig A. J. Fisher,  Akihide Kuwabara,  Yukio Sato,  Takao Shimizu,  Yosuke Hamasaki,  Hiroshi Takashima, and  Mitsuru Itoh




View Online



Export Citation



CrossMark



additive manufacturing epitaxial crystal growth cerium oxide polishing powder silver nanoparticles sputtering targets III-IV semiconductors CVD precursors europium phosphors

gallium lump glassy carbon nanodispersions InAs wafers laser crystals ultra high purity materials MOFs

surface functionalized nanoparticles organometallics quantum dot rare earth metals photovoltaics refractory metals MOCVD

superconductors transparent ceramics ultra high purity silicon

*American Elements opens up a world of possibilities so you can **Now Invent!***

Over 15,000 certified high purity laboratory chemicals, metals, & advanced materials and a state-of-the-art Research Center. Printable GHS-compliant Safety Data Sheets. Thousands of new products. And much more. All on a secure multi-language "Mobile Responsive" platform.

deposition slugs OLED Lighting spintronics solar energy

osmium nanoribbons thin films chalcogenides AuNPs

GDC Li-ion battery electrolytes 99.999% ruthenium spheres

endohedral fullerenes copper nanoparticles diamond micropowder

CIGS MBE grade materials palladium catalysts flexible electronics

pyrolytic graphite 3d graphene foam indium tin oxide mesoporous silica

raman substrates sapphire windows tungsten carbide InGaAs

barium fluoride carbon nanotubes lithium niobate scandium powder

perovskite crystals yttrium iron garnet alternative energy h-BN

gold nanocubes graphene oxide macromolecules photonics

rhodium sponge fiber optics beamsplitters infrared dyes zeolites

fused quartz metallocenes platinum ink buckyballs Ti-6Al-4V

Now Invent.TM

The Next Generation of Material Science Catalogs

www.americanelements.com



A computational search for wurtzite-structured ferroelectrics with low coercive voltages

Cite as: APL Mater. 8, 121102 (2020); doi: 10.1063/5.0023626

Submitted: 3 August 2020 • Accepted: 15 November 2020 •

Published Online: 7 December 2020



Hiroki Moriwake,^{1,a)} Rie Yokoi,¹ Ayako Taguchi,¹ Takafumi Ogawa,¹ Craig A. J. Fisher,¹ Akihide Kuwabara,¹ Yukio Sato,² Takao Shimizu,³ Yosuke Hamasaki,⁴ Hiroshi Takashima,⁵ and Mitsuru Itoh⁵

AFFILIATIONS

¹Nanostructures Research Laboratory, Japan Fine Ceramics Center, Nagoya 456-8587, Japan

²Department of Materials Science and Engineering, Kyushu University, Fukuoka 819-0395, Japan

³Research Center for Functional Materials, National Institute for Materials Science, Tsukuba 305-0047, Japan

⁴Department of Applied Physics, National Defense Academy, Yokosuka 239-8686, Japan

⁵Research Institute for Advanced Electronics and Photonics, National Institute of Advanced Industrial Science and Technology, Tsukuba 305-8568, Japan

^{a)} Author to whom correspondence should be addressed: moriwake@jfcc.or.jp

ABSTRACT

Ferroelectricity has recently been observed in wurtzite-structured Sc-doped AlN thin films, five years after our initial prediction of ferroelectricity in wurtzite compounds based on first-principles calculations. The thin films exhibited a much higher coercive voltage (3 MV/cm) than that of conventional perovskite-structured ferroelectric material PbTiO₃, however, making it difficult to switch the films' polarity and limiting their practical application. To identify tetrahedral ferroelectric materials with low coercive voltages, we have carried out a wider exploration of candidate binary compounds, from halides to chalcogenides to pnictogenides, using first-principles methods. The overall trend is for polarization switching barriers to decrease with decreasing anion-to-cation radius ratio, with the lowest barriers found in monovalent compounds such as the copper and silver halides; e.g., CuCl is calculated to have a switching barrier of 0.17 eV/f.u. and that of AgI is 0.22 eV/f.u., values similar in magnitude to that of PbTiO₃ (0.20 eV/f.u.). Applying an epitaxial tensile strain to the basal plane is also effective for lowering the potential barrier further, with barriers in both AgI and CuCl decreasing to 0.04 eV/f.u. when a 5% in-plane expansion is applied. The results suggest that tetrahedral ferroelectrics with moderate coercive voltages (below 100 kV/cm) should be achievable.

© 2020 Author(s). All article content, except where otherwise noted, is licensed under a Creative Commons Attribution (CC BY) license (<http://creativecommons.org/licenses/by/4.0/>). <https://doi.org/10.1063/5.0023626>

Ferroelectrics are materials possessing a spontaneous electric polarization, P_s , that can be switched between two or more symmetry-related variants by application of an electric field, E . Such compounds typically transform between polar (low symmetry) and non-polar (high symmetry) phases corresponding to ferroelectric and paraelectric states, respectively, as a function of temperature (or pressure). The wurtzite structure (S.G. $P6_3mc$) is non-centrosymmetric and thus stoichiometric binary compounds with this crystal type are polar [Fig. 1(a)]. Until recently, wurtzite-structured crystals were thought to be non-ferroelectric because of the difficulty of switching the cation-centered tetrahedra of which they are constituted, and earlier theoretical calculations examining

polarization and piezoelectricity in wurtzite crystals only considered displacement of the cations within the tetrahedra.^{1–5} However, as early as 1973, Sawada *et al.*⁶ traced the electric displacement–electric field (D – E) hysteresis loop of wurtzite BeO and measured a small polarization of 0.061 C/m² at 805 °C. Similarly, in 1996, when measuring the P – E hysteresis loop of Li-doped ZnO, Onodera *et al.*⁷ detected a dielectric anomaly at 330 K with a small polarization of 0.044 μ C/cm² at room temperature, and Joseph *et al.*⁸ in 1999 reported a dielectric anomaly at 340 K in the same material. Such observations motivated us to consider the possibility of wurtzite crystals exhibiting ferroelectricity by a reversal in orientation of the cation–anion tetrahedra.^{9,10} We showed using

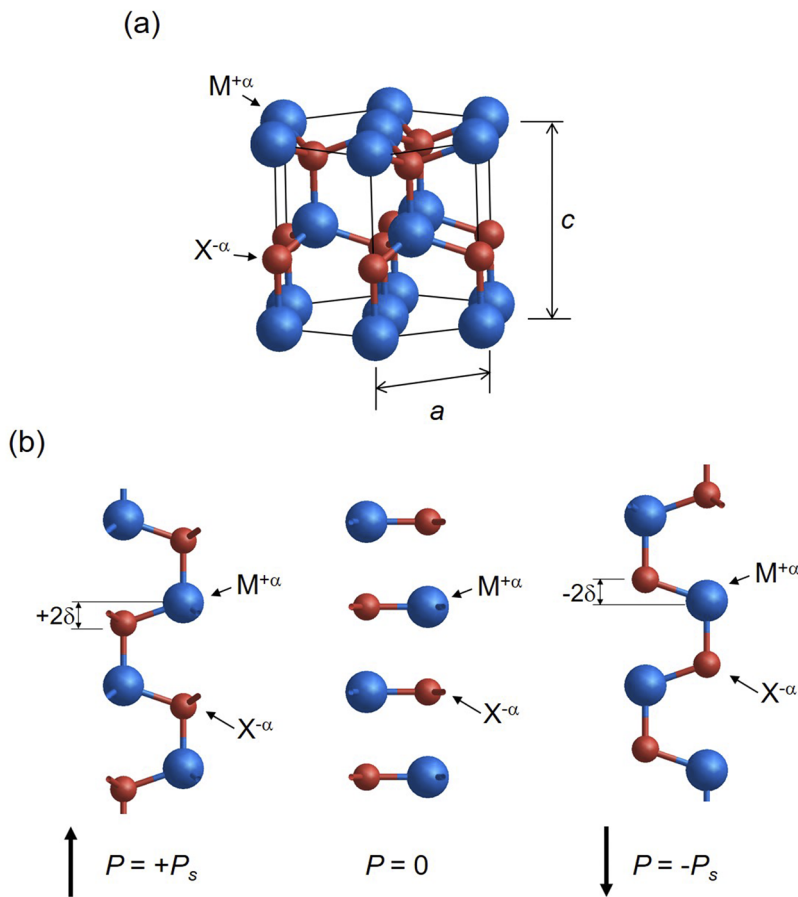


FIG. 1. (a) Hexagonal wurtzite structure of binary compound MX (space group $P6_3mc$). (b) Polarization switching mechanism: ferroelectric state with $P = +P_s$, paraelectric (intermediate) state with $P = 0$, and ferroelectric state with $P = -P_s$ after inversion of MX_4 tetrahedra by applying an electric field parallel to the c axis, where δ is displacement of an ion relative to its position in the intermediate structure.

first-principles calculations of Zn and Be chalcogenides that displacement of the cations relative to the anions parallel to the c axis produces a metastable centrosymmetric structure, which is paraelectric (space group $P6_3/mmc$) and halfway between the two polar structures of opposite tetrahedral orientation, as illustrated in Fig. 1(b); this intermediate state was demonstrated by Dreyer *et al.*¹¹ to be the correct reference structure for accurately calculating polarization constants. If the energy required for this displacement is sufficiently low, it should be possible to switch the polarization, thereby holding out the promise that ferroelectric materials consisting of tetrahedral networks, otherwise known as tetrahedral ferroelectrics, can be developed as an alternative to the conventional perovskite materials. A similar method was used by Bennett *et al.* to examine a large number of stuffed wurtzites.¹²

In the years since our initial theoretical study, a number of groups have performed experiments in an effort to demonstrate ferroelectricity in wurtzite crystals.^{13–22} In particular, in 2019, Fichtner *et al.*²³ reported a well-defined P – E hysteresis loop with a high spontaneous polarization of 1.00 C/m^2 in Sc-doped AlN thin films, their work providing further stimulus to the search for tetrahedral ferroelectrics. To be practical, a ferroelectric material requires a moderate-to-low coercive voltage, especially if it is to be used

in ferroelectric memory or similar devices, but the coercive voltage of their material was reported to be very high; at 2 MV/cm – 5 MV/cm , the coercive voltages of their Al(Sc)N thin films are around two orders of magnitude higher than those of conventional perovskite-type ferroelectric materials, such as BaTiO_3 (25 kV/cm)²⁴ and PbTiO_3 (121 kV/cm).²⁵ There is thus a strong impetus to discover new materials with coercive voltages $<100 \text{ kV/cm}$.

In our previous reports,^{9,10} we estimated the coercive voltages of a limited number of wurtzite-structured compounds by calculating activation energies for (homogeneous) polarization switching of tetrahedra. In this report, we expand our exploration of the compositional phase space to encompass a wider range of binary compounds, thereby identifying novel ferroelectrics with low coercive voltages. We began with compounds that have been experimentally confirmed to have the wurtzite structure, whether under standard or non-standard (high temperature, high pressure, nanosizing, and so on) conditions. Many of these compounds have their wurtzite polymorphs included in the International Crystal Structure Database,²⁶ viz., CuI, AgI, BeO, MgTe, MnO, MnS, ZnO, ZnS, ZnSe, CdS, CdSe, CdTe, AlN, GaN, InN, InSb, and 2H-SiC . For those whose wurtzite form has not been reported in detail (viz., CuCl, CuBr, BeS, MgS, MgSe, MnSe, MnTe, ZnTe, AlP, AlAs, AlSb, GaP, GaAs, GaSb, InP, and InAs), we used an analog structure containing the same

cation and substituted the appropriate X element to construct starting structures relaxed using first-principles methods. We also considered a number of hypothetical wurtzite-structured compounds, viz., AgCl, AgBr, BeSe, BeTe, MgO, and CdO, for comparison, their initial structures constructed in a similar way.

Similar to our earlier study, density functional theory (DFT) calculations, as implemented in VASP,^{27,28} were used to characterize each of the above compounds and assess their suitability as candidate tetrahedral ferroelectrics. All calculations were performed using the Perdew–Burke–Ernzerhof form of the generalized gradient approximation optimized for solids (GGA-PBESol) to treat

exchange–correlation interactions.²⁹ The plane wave basis projector augmented wave method³⁰ was used with 2s and 2p electrons for Be, N, O, C, and F, 3s and 3p electrons for Mg, Al, Si, P, S, and Cl, 4s and 4p electrons for As, Se, and Br, 5s and 5p electrons for In, Sb, Te, and I, and 3d and 4s electrons for Mn, Cu, and Zn treated as valence electrons. A plane wave cutoff energy of 550 eV was used in all cases. The convergence of the total energies with respect to cutoff energies up to 800 eV was better than 0.015 eV/f.u. Numerical integration was carried out using a Γ -centered 0.25 \AA^{-1} spaced k -point mesh, generated according to the Monkhorst–Pack scheme,³¹ within the first Brillouin zone of the four-atom wurtzite unit cell. To adjust

TABLE I. Calculated lattice parameters, bandgaps (E_{bg}), Born effective charges (Z^*_{33}), and spontaneous polarizations (P_s) of binary compounds examined in this study. Where available, experimental lattice parameters (in parentheses) and calculated deviations are also included.

Compd	a (Å)	Δa (%)	c (Å)	Δc (%)	z	Δz (%)	Reference	E_{bg} (eV)	Z^*_{33}	P_s (C/m ²)
CuCl	3.723		6.190		0.368			0.8	1.12	0.40
CuBr	3.941		6.498		0.372			0.7	1.26	0.38
CuI	4.191(4.310)	−2.76	6.902(7.090)	−2.65	0.373(0.375)	−0.53	37	1.4	1.01	0.27
AgCl	4.194		6.678		0.384			1.2	1.21	0.30
AgBr	4.356		7.029		0.379			1.2	1.28	0.30
AgI	4.557(4.592)	−0.76	7.450(7.510)	−0.80	0.375(0.375)	0.00	38	1.4	1.22	0.27
BeO	2.695(2.696)	−0.04	4.377(4.379)	−0.05	0.378(0.378)	0.00	39	7.5	1.85	1.15
BeS	3.414		5.628		0.374			3.5	1.63	0.65
BeSe	3.620		5.971		0.374			3.2	1.56	0.56
BeTe	3.953		6.528		0.373			2.1	1.31	0.39
MgO	3.298		5.022		0.397			3.6	1.90	0.67
MgS	4.026		6.419		0.382			3.6	1.96	0.53
MgSe	4.219		6.784		0.380			2.8	1.96	0.49
MgTe	4.565(4.531)	0.75	7.406(7.350)	0.76	0.377(0.375)	0.53	40	2.6	1.98	0.43
MnO	3.450(3.372)	2.31	5.311(5.386)	1.39	0.393(0.365)	7.67	41	0	2.08	0.69
MnS	4.029(3.987)	1.05	6.445(6.438)	0.11	0.381(0.375)	1.60	42	1.0	2.04	0.55
MnSe	4.218		6.787		0.379			0.5	2.07	0.52
MnTe	4.523		7.351		0.377			0.9	1.99	0.44
ZnO	3.237(3.249)	−0.37	5.227(5.205)	0.42	0.379(0.382)	−0.79	43	0.8	2.19	0.94
ZnS	3.785(3.823)	−0.99	6.213(6.261)	−0.77	0.374(0.375)	−0.27	44	2.5	2.01	0.65
ZnSe	3.981(3.996)	−0.38	6.542(6.626)	−1.27	0.374(0.375)	−0.27	45	1.6	2.09	0.61
ZnTe	4.281		7.050		0.373			1.9	2.03	0.52
CdO	3.635		5.693		0.389			0.5	2.27	0.71
CdS	4.133(4.137)	−0.10	6.724(6.716)	0.12	0.377(0.377)	0.00	46	1.4	2.24	0.60
CdSe	4.311(4.298)	0.30	7.035(7.008)	0.39	0.376(0.376)	0.00	47	1.2	2.43	0.60
CdTe	4.589(4.566)	0.50	7.523(7.502)	0.28	0.375(0.375)	0.00	48	1.5	2.30	0.51
AlN	3.114(3.111)	0.10	4.983(4.998)	−0.30	0.382(0.385)	−0.78	49	4.2	2.68	1.21
AlP	3.861		6.339		0.375			1.9	2.34	0.73
AlAs	4.008		6.589		0.374			1.7	2.25	0.65
AlSb	4.350		7.159		0.374			1.0	1.90	0.47
GaN	3.181(3.189)	−0.25	5.184(5.185)	−0.04	0.377(0.379)	−0.53	50	2.5	2.74	1.24
GaP	3.832		6.317		0.374			1.4	2.19	0.69
GaAs	3.991		6.578		0.374			0.5	2.32	0.68
GaSb	4.310		7.101		0.374			0.1	2.38	0.60
InN	3.538(3.538)	0.00	5.717(5.704)	0.23	0.379(0.377)	0.53	51	0.6	3.01	1.08
InP	4.149		6.808		0.375			0.9	2.69	0.72
InAs	4.298		7.060		0.374			0.5	2.54	0.64
InSb	4.598(4.560)	0.83	7.568(7.460)	1.45	0.374(0.350)	6.86	52	0.7	2.17	0.48
SiC	3.077(3.079)	−0.06	5.050(5.053)	−0.06	0.376(0.376)	0.00	53	1.9	2.87	1.39

for the known underestimation of electronic bandgaps in transition metal-containing compounds using the GGA method, a Hubbard U term³² of $U_{\text{eff}} = 3.6$ eV was added in the case of Mn-containing compounds.³³

Atom positions and lattice parameters of each unit cell were relaxed until residual forces were smaller than 0.005 eV/Å. Born effective charge tensors were calculated using the Berry phase approach within density functional perturbation theory.³⁴ Spontaneous polarizations, P_s , were calculated as the difference in polarization between paraelectric and ferroelectric structures, where polarization P induced by periodic displacement δ of atoms relative to their positions in the non-polar centrosymmetric ($P6_3/mmc$) structure is related to the Born effective charge of the cation in the c direction, Z_{33}^* , and the volume of the unit cell, V , according to the following equation:

$$P = \frac{Z_{33}^* \delta}{V}. \quad (1)$$

Calculated lattice parameters, bandgaps (E_g), Z_{33}^* , and P_s of each compound are compared with available experimental data in Table I. The calculated lattice parameters reproduce the experimental data well and are within the usual DFT error, validating the use of PBEsol potentials for modeling ferroelectric transformations.

In addition to a low coercive voltage, conventional ferroelectric materials also need to be electronically insulating, i.e., have sufficiently wide bandgaps, to undergo switching by an applied electric field. Although DFT calculations using GGA functionals are known to underestimate bandgaps significantly, all compounds apart from MnO exhibited non-zero E_g values and thus should be electronic insulators in their polar forms. Because of its lack of bandgap, even with a Hubbard U term included, MnO was not considered further. In addition, AlAs, AlSb, GaP, GaAs, GaSb, InP, InAs, and InSb were each calculated to have a metallic band structure in their non-polar (transition) state, so these compounds are likely unsuitable for use as ferroelectric materials according to the modern theory of polarization.^{35,36}

Unlike in typical perovskite ferroelectric compounds, the calculated Z_{33}^* values of each ion in most cases deviated only slightly from their nominal charges. All compounds exhibited relatively large P_s values, with trivalent compounds having the largest (e.g., 1.24 C/m² for GaN and 1.21 C/m² for AlN), consistent with the magnitudes of their Born effective charges being around 3. In contrast, monovalent compounds were calculated to have relatively small polarizations (e.g., 0.27 C/m² for CuI and 0.27 C/m² for AgI) with small Born effective charges of around +1 and −1 for cations and anions, respectively. Despite this, P_s values for these monovalent compounds were found to be similar in magnitude to that of perovskite BaTiO₃ (0.25 C/m²) as a result of the large displacement of their cations and anions from the centrosymmetric positions.

In many ferroelectrics, polarization switching may occur by more complicated (inhomogeneous) processes, such as domain nucleation and growth (typically around defects) or order–disorder processes. Although it is possible to construct models encompassing these more complex phenomena, they require tailoring to each particular material and are thus time-consuming

and computationally expensive, which is impractical in terms of developing an efficient materials exploration method. For the purposes of this study, we have thus assumed a direct switching mechanism, with the coercive field estimated by calculating the magnitude of the polarization switching potential, E_{sw} , from DFT energies of the crystal structure in various states between the polar variants using the fixed displacement-field (or fixed D-field) method.^{54,55} This may mean that the coercive fields are overestimated in some cases, but it has the merit of revealing trends within a reasonable time frame, thereby providing insight into which materials are promising as tetrahedral ferroelectrics. Efforts to determine the precise details of the switching mechanism can then be focused on those systems, which exhibit interesting ferroelectric behavior.

The calculated potential surfaces from which E_{sw} values were extracted are plotted in Figs. 2–4 for monovalent compounds (Cu and Ag halides), divalent compounds (Be, Mg, Mn, Zn,

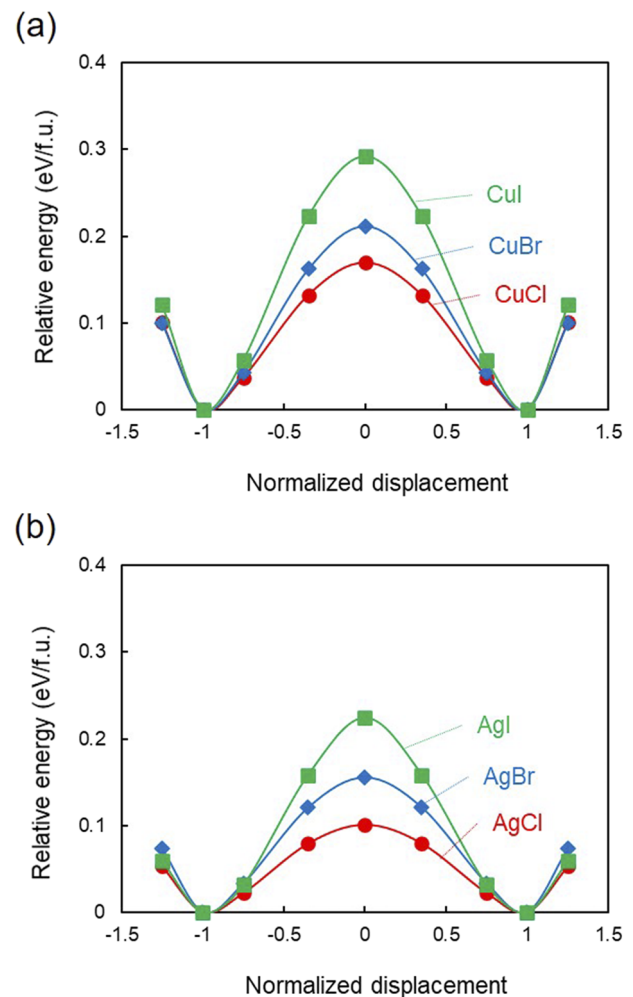


FIG. 2. Calculated potential surfaces for ferroelectric cation displacement in monovalent halides: (a) CuX and (b) AgX for X = Cl, Br, and I.

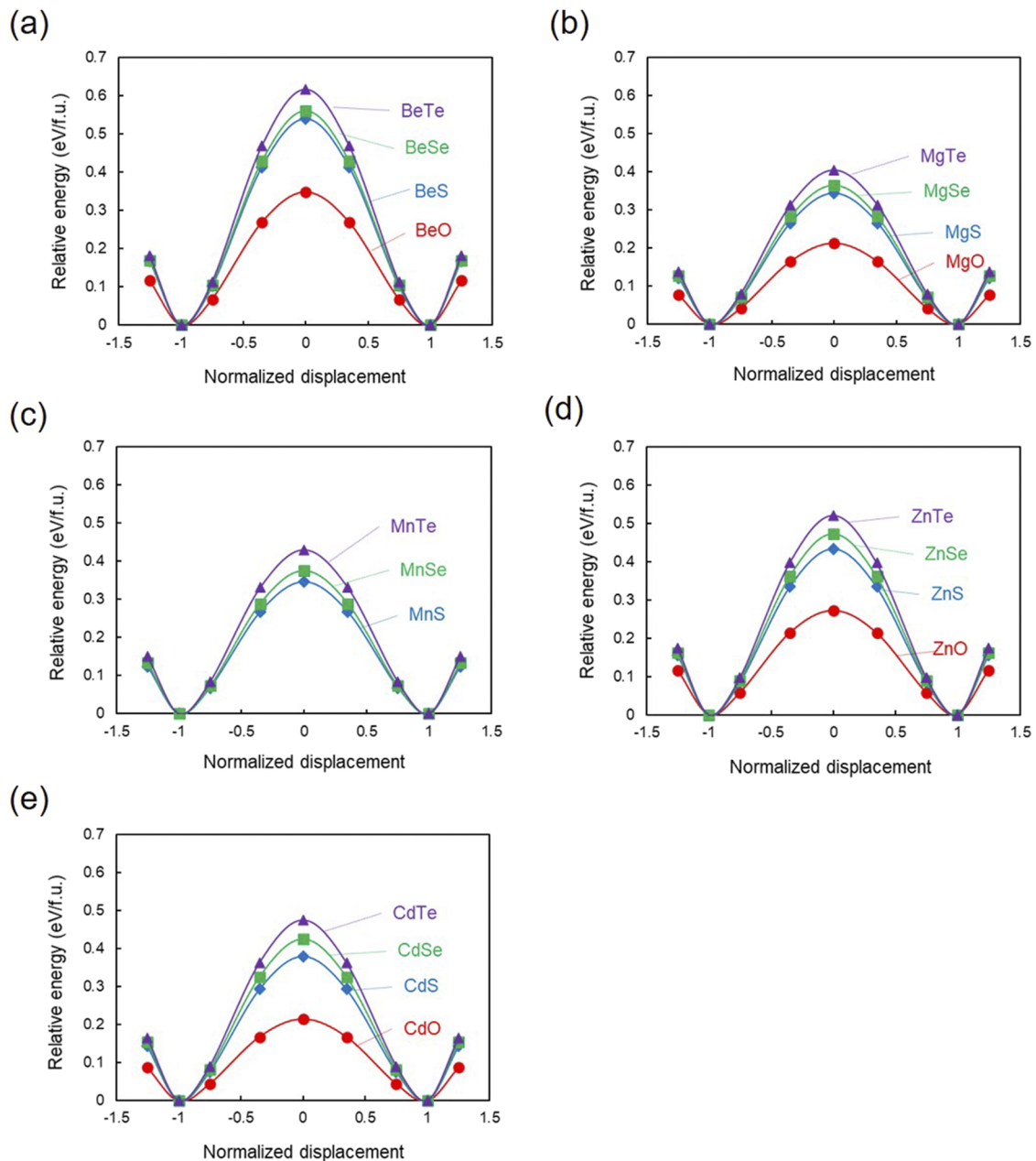


FIG. 3. Calculated potential surfaces for ferroelectric cation displacement in divalent chalcogenides: (a) BeX, (b) MgX, (c) MnX, (d) ZnX, and (e) CdX for X = O, S, Se, and Te. MnO is excluded because it is electronically conductive.

and Cd chalcogenides), and trivalent compounds (Al, Ga, and In pnictogenides and 2H-SiC), respectively (results for compounds with electronically conducting paraelectric phases are included for completeness). The results reveal that all compounds exhibit a double-well potential, with the maximum corresponding to the intermediate non-polar state between the minima of the two polar variants. Out of all the compounds examined, the monovalent

compounds (Cu and Ag halides) have the lowest E_{sw} values, viz., 0.17 eV/f.u. for CuCl, 0.21 eV/f.u. for CuBr, 0.29 eV/f.u. for CuI, 0.11 eV/f.u. for AgCl, 0.15 eV/f.u. for AgBr, and 0.22 eV/f.u. for AgI. These barriers are close in magnitude to that of ferroelectric perovskite PbTiO_3 at 0.2 eV/f.u.⁵⁶ In all cases, the potential barrier decreases with decreasing atomic number (thus ion radius) of the anion.

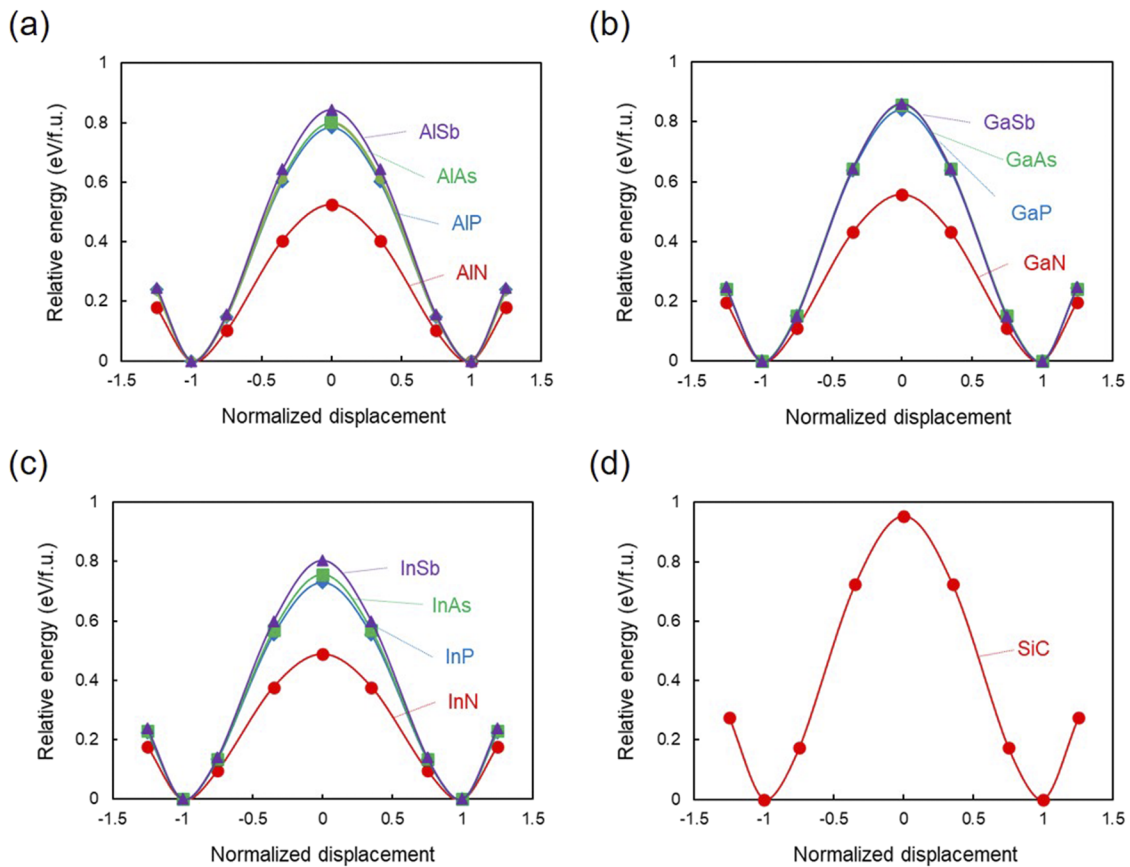


FIG. 4. Calculated potential surfaces for ferroelectric cation displacement in trivalent pnictogenides and silicon carbide: (a) AlX, (b) GaX, (c) InX for X = N, P, As, and Sb and (d) 2H-SiC.

Figure 5 shows a plot of E_{sw} vs anion/cation radius ratio, χ ($=r_{anion}/r_{cation}$), using Shannon's ionic radii⁵⁷ in sixfold coordination where available. In the case of anions N^{3-} and P^{3-} for which ionic radii are only reported for fourfold coordination, radii were

estimated using the ratio of Madelung constants for wurtzite and rock-salt structures with a Born exponent of 6 and 8, respectively.⁵⁸ In this figure, compounds that have the wurtzite structure under standard conditions are labeled in bold and in boxes; compounds

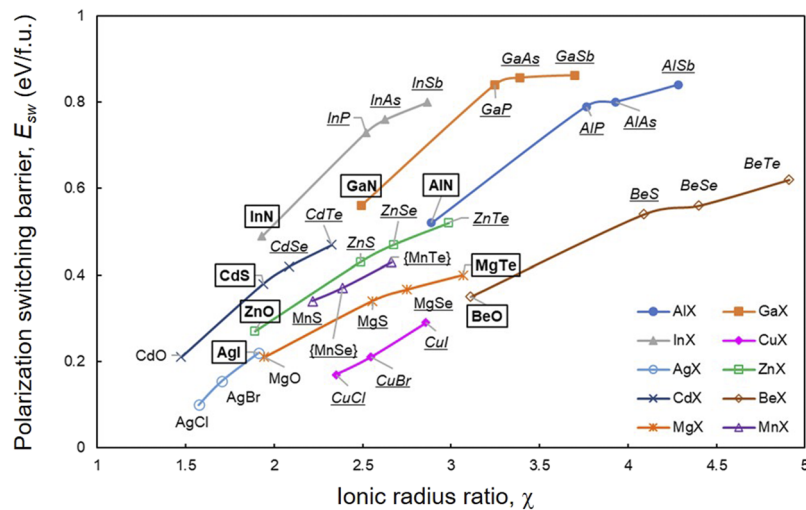


FIG. 5. Relationship between polarization switching barrier, E_{sw} , and ionic radius ratio, $\chi = r_{anion}/r_{cation}$. Compounds with the wurtzite structure under standard conditions are labeled in bold within boxes, those with the zinc blende structure in italics, those with the nickeline structure in curly brackets, and those with the rock-salt structure in normal font. Compounds known to be synthesizable in the wurtzite structure under non-equilibrium or non-standard conditions are underlined.

whose ground state is the zinc blende structure are labeled in italics, those with the nickeline (NiAs) structure in curly brackets, and those with the rock-salt structure in normal style. Compounds that have been reported to be prepared in the wurtzite form under non-equilibrium conditions are underlined. For example, both of the nickeline-type compounds, MnSe and MnTe, have been stabilized with the wurtzite structure when prepared in nanowire, nanoribbon, or nanoparticle form.^{59,60} The results show that, for both hypothetical and actual wurtzites, there is a comparatively simple relationship between χ and E_{sw} over a wide range of chemical compositions, with E_{sw} increasing monotonically with increasing χ . Deviations from linearity can be ascribed to differences in the nature of the chemical bonding (from ionic to covalent), especially at higher χ values beyond the normal range of ground-state wurtzite compounds (roughly $1.9 \lesssim \chi \lesssim 3.1$).

We rationalize the linear relationship between E_{sw} and χ as follows: A decrease in χ means that structures with sixfold coordinated sites (e.g., the rock-salt structure) become more stable compared to structures with fourfold coordinated sites such as wurtzite compounds so that the energy difference between polar variants ($P6_3mc$) and the non-polar ($P6_3/mmc$) state, i.e., E_{sw} , decreases; in other

words, the non-polar state becomes energetically more favorable. When $\chi \lesssim 1.9$, the rock-salt ($Fm\bar{3}m$) structure is the most stable, as found for AgCl, AgBr, CdO, and MgO. In terms of phase stability, the MnX compounds are the most different to the others, which we posit is a result of the markedly different bonding states associated with the d-orbital electrons of Mn^{2+} ions. MgS also appears to be an anomaly, having the rock-salt structure at room temperature, although it has been shown to take on the wurtzite structure in thin-film form.⁶¹ In regard to compounds with low switching barriers, CuCl lies just within the wurtzite zone; experimentally, it is reported to have the zincblende structure ($F43m$) but transforms to wurtzite at around 400 °C,⁶² making it a good candidate for being a tetrahedral ferroelectric if prepared under suitable synthesis conditions. According to our DFT calculations, the energy difference between wurtzite CuCl and zincblende CuCl is as little as 1.4 meV/f.u. In contrast, for the well-known rock-salt-structured compound AgCl, $\chi_{AgCl} = 1.6$, which is well outside the wurtzite zone, and so is predicted to be very difficult to stabilize in wurtzite form, in good agreement with experiment. Indeed, the energy difference between rock-salt AgCl and wurtzite AgCl 29 meV/f.u.) is much larger than that between the analogous forms of CuCl.

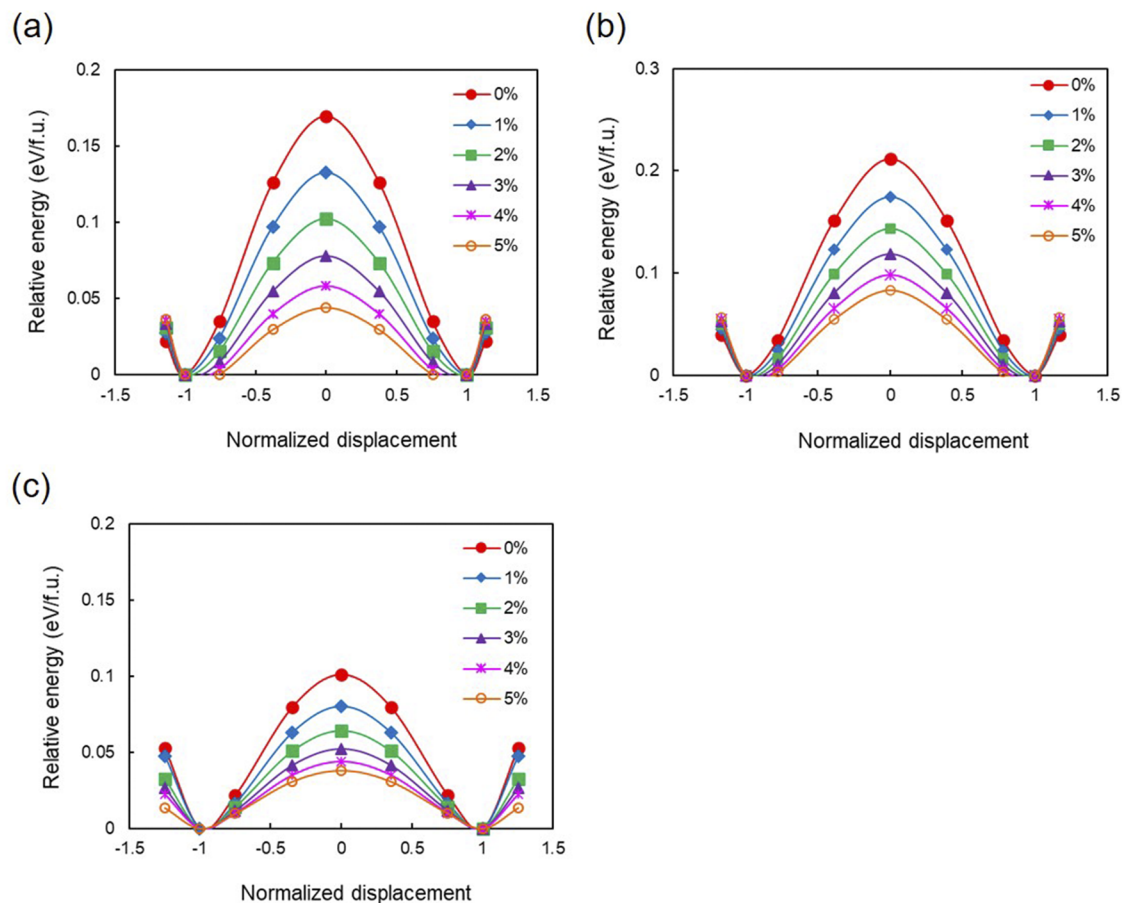


FIG. 6. Effect of *ab* epitaxial strain (in %) on the ferroelectric potential barrier in wurtzite-structured (a) CuCl, (b) CuBr, and (c) AgCl.

As argued in our earlier paper,¹⁰ one effective method of lowering the switching barrier is application of an epitaxial strain to expand the crystal in the basal plane, (0001). This was also found to be the case for all compounds examined in this study. As an example, results for CuCl, CuBr, and AgCl are shown in Fig. 6. Applying a 5% epitaxial strain is seen to reduce the potential barrier from 0.17 eV/f.u. to 0.04 eV/f.u., 0.21 eV/f.u. to 0.08 eV/f.u., and 0.22 eV/f.u. to 0.09 eV/f.u. for CuCl, CuBr, and AgCl, respectively. These low potential barriers are similar to those of conventional perovskite ferroelectrics (e.g., BaTiO₃ at 0.02 eV/f.u.⁵⁶). A low coercive voltage (below 100 kV/cm) should thus be realizable in strained thin films of these compounds. In terms of substrates, hexagonal ScAlMgO₄ is one promising candidate because it is often used as the substrate for hetero-epitaxial growth of wurtzite-structured ZnO thin films on account of the very small in-plane (0001) lattice mismatch.⁶³ As cations in ScAlMgO₄ can be substituted with a large variety of isovalent cations (e.g., Y³⁺ or In³⁺ for Sc³⁺, Ga³⁺ or Fe³⁺ for Al³⁺, and Zn²⁺, Mn²⁺, Co²⁺, or Cu²⁺ for Mg²⁺), it should be possible to tailor the lattice parameters of the substrate to high precision to induce a suitable epitaxial strain in the thin film.

In summary, we carried out a systematic examination of binary compounds in the search for novel tetrahedral ferroelectrics, specifically those with the wurtzite structure and low coercive voltage, using first-principles calculation methods. Three main conclusions can be drawn:

- (1) Of the wurtzite-structured binary compounds examined, the two lowest polarization switching barriers found were 0.11 eV/f.u. in AgCl and 0.15 eV/f.u. in AgBr, but both these compounds are highly stable in the rock-salt structure. The third lowest was 0.17 eV/f.u. in CuCl, which normally has a zinc-blende structure, which is only slightly more stable than the wurtzite structure. This potential barrier is similar in magnitude to that of ferroelectric perovskite PbTiO₃, suggesting that CuCl will have a low coercive voltage if prepared in wurtzite form. Wurtzite-structured AgI and CuBr, with barriers of 0.22 eV/f.u., also appear to be promising tetrahedral ferroelectrics.
- (2) The polarization switching barrier decreases with decreasing anion-cation radii ratio, $r_{\text{anion}}/r_{\text{cation}}$. This is related to the decreased stability of cation-anion tetrahedra as anions become smaller and cations larger, reducing the energy difference between polar variants (with $P6_3mc$ symmetry) and the non-polar state (with $P6_3/mmc$ symmetry).
- (3) Applying an epitaxial tensile strain in the (0001) plane is effective at lowering the potential barrier for polarization switching. In wurtzite-structured CuCl, the potential barrier decreased from 0.17 eV/f.u. to 0.04 eV/f.u. after expanding the crystal 5% parallel to (0001). Low coercive voltages (below 100 kV/cm) should thus be realizable by synthesizing this compound as a thin film with epitaxial strains of a few percent.

This work was supported by the Ministry of Education, Culture, Sports, Science and Technology of Japan through the Grants-in-Aid for Scientific Research (A) (Grant No. JP20H00314) and the Murata Science Foundation.

DATA AVAILABILITY

The data that support the findings of this study are available within the article.

REFERENCES

- ¹A. Dal Corso, M. Posternak, R. Resta, and A. Baldereschi, *Phys. Rev. B* **50**, 10715 (1994).
- ²S. Massidda, R. Resta, M. Posternak, and A. Baldereschi, *Phys. Rev. B* **52**, R16977 (1995).
- ³F. Bernardini, V. Fiorentini, and D. Vanderbilt, *Phys. Rev. B* **56**, R10024 (1997).
- ⁴Y. Uetsuji, E. Nomura, K. Koike, S. Sasa, M. Inoue, and M. Yano, *J. Soc. Mater. Sci., Jpn.* **58**, 243 (2009).
- ⁵F. Bernardini, V. Fiorentini, and D. Vanderbilt, *Phys. Rev. B* **63**, 193201 (2001).
- ⁶S. Sawada, S. Hirotsu, H. Iwamura, and Y. Shiroishi, *J. Phys. Soc. Jpn.* **35**, 946 (1973).
- ⁷A. Onodera, N. Tamaki, Y. Kawamura, T. Sawada, and H. Yamashita, *Jpn. J. Appl. Phys., Part 1* **35**, 5160 (1996).
- ⁸M. Joseph, H. Tabata, and T. Kawai, *Appl. Phys. Lett.* **74**, 2534 (1999).
- ⁹H. Moriwake, A. Konishi, T. Ogawa, K. Fujimura, C. A. J. Fisher, A. Kuwabara, T. Shimizu, S. Yasui, and M. Itoh, *Appl. Phys. Lett.* **104**, 242909 (2014).
- ¹⁰A. Konishi, T. Ogawa, C. A. J. Fisher, A. Kuwabara, T. Shimizu, S. Yasui, M. Itoh, and H. Moriwake, *Appl. Phys. Lett.* **109**, 102903 (2016).
- ¹¹C. E. Dreyer, A. Janotti, C. G. Van de Walle, and D. Vanderbilt, *Phys. Rev. X* **6**, 021038 (2016).
- ¹²J. W. Bennett, K. F. Garrity, K. M. Rabe, and D. Vanderbilt, *Phys. Rev. Lett.* **109**, 167602 (2012).
- ¹³R. Deng, K. Jiang, and D. Gall, *J. Appl. Phys.* **115**, 013506 (2014).
- ¹⁴P. M. Mayrhofer, H. Riedl, H. Euchner, M. Stöger-Pollach, P. H. Mayrhofer, A. Bittner, and U. Schmid, *Acta Mater.* **100**, 81 (2015).
- ¹⁵C. Tholander, J. Birch, F. Tasnádi, L. Hultman, J. Pališaitis, P. O. Å. Persson, J. Jensen, P. Sandström, B. Alling, and A. Žukauskaitė, *Acta Mater.* **105**, 199 (2016).
- ¹⁶M. Uehara, H. Shigemoto, Y. Fujio, T. Nagase, Y. Aida, K. Umeda, and M. Akiyama, *Appl. Phys. Lett.* **111**, 112901 (2017).
- ¹⁷J. Maiz, P. Loxq, P. Fau, K. Fajerwerger, M. L. Kahn, G. Fleury, G. Hadziioannou, G. Guegan, J. Majimel, M. Maglione, V. Rodriguez, and E. Pavlopoulou, *J. Phys. Chem. C* **123**, 29436 (2019).
- ¹⁸M. Noor-A-Alam, O. Z. Olszewski, and M. Nolan, *ACS Appl. Mater. Interfaces* **11**, 20482 (2019).
- ¹⁹A. Samantaa, M. N. Goswami, and P. K. Mahapatra, *Mater. Sci. Eng. B* **245**, 1 (2019).
- ²⁰W. Zhang and Z. Fan, *Phys. Status Solidi RRL* **13**, 1800584 (2019).
- ²¹N. Singh and P. Singh, *RSC Adv.* **10**, 11382 (2020).
- ²²M. Atif, U. Younas, W. Khalid, Z. Ahmed, Z. Ali, and M. Nadeem, *J. Mater. Sci.: Mater. Electron.* **31**, 5253 (2020).
- ²³S. Fichtner, N. Wolff, F. Lofink, L. Kienle, and B. Wagner, *J. Appl. Phys.* **125**, 114103 (2019).
- ²⁴T. Hayashi, N. Ohji, K. Hirohara, T. Fukunaga, and H. Maiwa, *Jpn. J. Appl. Phys., Part 1* **32**, 4092 (1993).
- ²⁵F. M. Pontes, J. H. G. Rangel, E. R. Leite, E. Longo, J. A. Varela, E. B. Araújo, and J. A. Eiras, *Thin Solid Films* **366**, 232 (2000).
- ²⁶D. Zagorac, H. Müller, S. Ruehl, J. Zagorac, and S. Rehme, *J. Appl. Crystallogr.* **52**, 918 (2019).
- ²⁷G. Kresse and J. Furthmüller, *Phys. Rev. B* **54**, 11169 (1996).
- ²⁸G. Kresse and D. Joubert, *Phys. Rev. B* **59**, 1758 (1999).
- ²⁹J. P. Perdew, K. Burke, and M. Ernzerhof, *Phys. Rev. Lett.* **77**, 3865 (1996).
- ³⁰P. E. Blöchl, *Phys. Rev. B* **50**, 17953 (1994).
- ³¹H. J. Monkhorst and J. D. Pack, *Phys. Rev. B* **13**, 5188 (1976).
- ³²S. L. Dudarev, G. A. Botton, S. Y. Savrasov, C. J. Humphreys, and A. P. Sutton, *Phys. Rev. B* **57**, 1505 (1998).

- ³³F. Zhou, M. Cococcioni, C. A. Marianetti, D. Morgan, and G. Ceder, *Phys. Rev. B* **70**, 235121 (2004).
- ³⁴X. Wu, D. Vanderbilt, and D. R. Hamann, *Phys. Rev. B* **72**, 035105 (2005).
- ³⁵N. A. Spaldin, *J. Solid State Chem.* **195**, 2 (2012).
- ³⁶N. A. Benedek and T. Birol, *J. Mater. Chem. C* **4**, 4000 (2016).
- ³⁷J. Krug and L. Sieg, *Z. Naturforsch., A* **7**, 369 (1952).
- ³⁸G. Burley, *J. Chem. Phys.* **38**, 2807 (1963).
- ³⁹R. M. Hazen and L. W. Finger, *J. Appl. Phys.* **59**, 3728 (1986).
- ⁴⁰W. H. Zachariasen, *Z. Phys. Chem.* **128**, 417 (1927).
- ⁴¹K. M. Nam, Y.-I. Kim, Y. Jo, S. M. Lee, B. G. Kim, R. Choi, S.-I. Choi, H. Song, and J. T. Park, *J. Am. Chem. Soc.* **134**, 8392 (2012).
- ⁴²L. Corliss, N. Elliott, and J. Hastings, *Phys. Rev.* **104**, 924 (1956).
- ⁴³H. Sowa and H. Ahsbahs, *J. Appl. Crystallogr.* **39**, 169 (2006).
- ⁴⁴E. H. Kisi and M. M. Elcombe, *Acta Crystallogr. C* **45**, 1867 (1989).
- ⁴⁵I. V. Korneeva, *Kristall* **6**, 630 (1961).
- ⁴⁶H. Sowa, *Solid State Sci.* **7**, 73 (2005).
- ⁴⁷H. Sowa, *Solid State Sci.* **7**, 1384 (2005).
- ⁴⁸K. Ohata, J. Saraie, and T. Tanaka, *Jpn. J. Appl. Phys., Part 1* **12**, 1198 (1973).
- ⁴⁹J. Wang, M. Zhao, S. F. Jin, D. D. Li, J. W. Yang, W. J. Hu, and W. J. Wang, *Powder Diffr.* **29**, 352 (2014).
- ⁵⁰W. Paszkowicz, S. Podsiadlo, and R. Minikayev, *J. Alloys Compd.* **382**, 100 (2004).
- ⁵¹W. Paszkowicz, R. Černý, and S. Krukowski, *Powder Diffr.* **18**, 114 (2003).
- ⁵²S. A. Semiletov and M. Rozsibal, *Sov. Phys. Crystallogr.* **2**, 281 (1957).
- ⁵³H. Schulz and K. H. Thiemann, *Solid State Commun.* **32**, 783 (1979).
- ⁵⁴M. Stengel, N. A. Spaldin, and D. Vanderbilt, *Nat. Phys.* **5**, 304 (2009).
- ⁵⁵M. Stengel, D. Vanderbilt, and N. A. Spaldin, *Phys. Rev. B* **80**, 224110 (2009).
- ⁵⁶R. E. Cohen, *Nature* **358**, 136 (1992).
- ⁵⁷R. D. Shannon, *Acta Crystallogr. A* **32**, 751 (1976).
- ⁵⁸J. E. Huheey, E. A. Keiter, and R. L. Keiter, *Inorganic Chemistry*, 4th ed. (Harper Collins, New York, USA, 1993).
- ⁵⁹Y. Jiang, X.-M. Meng, W.-C. Yiu, J. Liu, J.-X. Ding, C.-S. Lee, and S.-T. Lee, *J. Phys. Chem. B* **108**, 2784 (2004).
- ⁶⁰S. Siol, Y. Han, J. Mangum, P. Schulz, A. M. Holder, T. R. Klein, M. F. A. M. van Hest, B. Gorman, and A. Zakutayev, *J. Mater. Chem. C* **6**, 6297 (2018).
- ⁶¹Y. H. Lai, Q. L. He, W. Y. Cheung, S. K. Lok, K. S. Wong, S. K. Ho, K. W. Tam, and I. K. Sou, *Appl. Phys. Lett.* **102**, 171104 (2013).
- ⁶²N. Zakharov, V. A. Klyuev, T. V. Zakharova, Yu. P. Toporov, and M. R. Kiselev, *Russ. J. Phys. Chem.* **75**, 415 (2001).
- ⁶³A. Ohtomo, K. Tamura, and K. Saikusa, *Appl. Phys. Lett.* **75**, 2635 (1999).